

VALIDATION OF URANS AND STRUCT- ϵ TURBULENCE MODELS FOR STRATIFIED SODIUM FLOW

Ralph Wisser, Emilio Baglietto

Department of Nuclear Science and Engineering
Massachusetts Institute of Technology
77 Mass Ave, Cambridge, MA 02108
rwisser@mit.edu

James Schneider, Mark H Anderson

Department of Mechanical Engineering
University of Wisconsin-Madison

ABSTRACT

Simulations of a transient stratified sodium experiment are carried out using a classic unsteady RANS model and the second-generation URANS model, STRUCT- ϵ . Turbulence modeling challenges and their implications to stratified flow prediction are discussed in the context of other sources of error. Input errors are discussed and addressed; discretization error is calculated to be less than 5% of the inlet velocity, for 80% of the domain; and remaining errors in temperature distributions are attributed to the turbulence model. Qualitative flow features from the simulations are presented and discussed. Compared to the experiment, the STRUCT- ϵ turbulence model provides a more physically accurate prediction of temperature and momentum mixing in key regions of the domain. Quantitative measures such as the L_2 norm of the temperature discrepancy demonstrate the improved performance of the STRUCT- ϵ approach. The magnitude of the temperature fluctuations is very well-predicted by the STRUCT- ϵ , while URANS overpredicts them by approximately 50%.

KEYWORDS

Stratification, turbulence modeling, model error

1. INTRODUCTION

The global focus on low-carbon energy technology has spurred interest in advanced nuclear reactors. Energy markets demand low-cost, technically-ready reactor designs, and liquid metal cooled nuclear reactors can meet these needs. Consequently, corporations and governments have poured new investments into metal-cooled reactors, from MYRRHA in Europe [1] to the Westinghouse Lead Cooled Fast Reactor [2] and Natrium in the United States [3]. To license, demonstrate, and commercialize these designs, the vendors require increased confidence in their computational engineering tools. Computational fluid dynamics (CFD) can play a significant role and greatly reduce the need for costly full-scale experiments.

CFD methods have a fundamentally stronger physical basis than legacy design tools such as system and subchannel codes. By discretizing and solving the governing equations over the entire domain, CFD has the potential to provide generally accurate predictions of pressure drop, temperature distribution, and other design metrics. But CFD predictions are a relatively coarse approximation of the true turbulent flow solution. The finer scales of turbulence are commonly not resolved, and the engineer relies on a

turbulence model to approximate their effects. For complex flow configurations with challenging physics, the turbulence model is often the largest source of error in the CFD prediction [4].

Engineers who leverage CFD methods for liquid metal cooled reactor design will have to balance the computational cost of their simulations against accuracy and uncertainty. This means using a turbulence model that is accurate, and generally applicable on any varying computational grids, while providing quantitative estimates of error. Generations of model developers have focused on advancing turbulence model accuracy, and recently methods have also been proposed to predict the error introduced by the turbulence model [4, 5, 6, 7, 8].

This paper assesses the applicability of state-of-the-art turbulence modeling on a challenging metal-cooled reactor prototypic flow. Stratification in liquid metal pools is a phenomenon caused by uneven heating or cooling of an open volume of fluid. This behavior occurs, for example, in the upper pool of a sodium fast cooled reactor (SFR). Predicting temperature distributions in stratified pools is an important requirement for CFD, and directly supports the design optimization and regulatory licensing of metal cooled reactors.

This work explores the accuracy of temperature predictions in liquid sodium stratified flow by comparing CFD predictions with experimental measurements. An anisotropic unsteady RANS (URANS) and a second-generation hybrid turbulence model named STRUCT- ϵ are assessed against the experimental measurements. The CFD error is quantitatively compared to provide an indication of model error in stratified flows and to support future efforts to quantitatively predict turbulence model error.

2. MODELING CHALLENGES

Stratification in sodium pools is a complex, 3D mixing phenomenon that challenges engineering models. This section describes the prototypic flow configuration and the modeling challenges it presents.

2.1 Experimental Apparatus

The experimental setup [9] provides detailed 3D temperature measurements in a stratified sodium pool. The apparatus includes a liquid sodium test section heated to 200-300°C. At the start of the test, valves open to inject cooler liquid sodium from a supply reservoir through three inlets at the base of the test section. In the upper region of the test section, sodium exits through two opposite openings, and flows down to a holding tank. The apparatus schematic is presented in Figure 1.

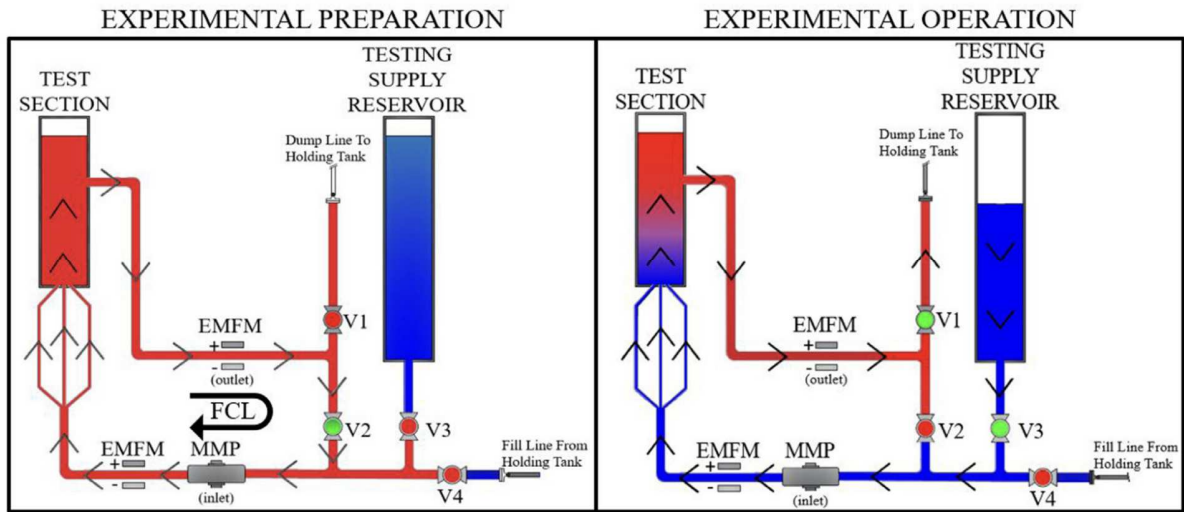


Figure 1: Experimental setup showing major components, the initial configuration, and the test operation schematic [9]

As the cool sodium flows through three jets into the test section base, hot and cold fluid mix. In the lower part of the domain vigorous turbulent mixing occurs, since interacting jets have been demonstrated to produce significant momentum mixing in previous liquid sodium experiments [10]. Higher in the domain, above the test section outlets, the fluid is expected to stratify as there is no bulk fluid flow through this region.

2.2 Sources of Error

Three major sources of error are present in the CFD stratification simulation and are described briefly. Input error relates to discrepancies between the simulation and experiment configurations, such as geometrical differences and simulation boundary assumptions. Numerical error is the result of the numerical solution and finite discretization of the continuous governing equations. The Computational Setup section includes quantitative estimations of numerical error. Finally, model error describes the discrepancy caused by inadequacies in the equations used to describe the underlying physics.

Inputs such as geometry and liquid sodium flow rate are described in the experiment description [9]. The experimental campaign comprises thirty-six separate experiments, with condition ranges listed in Table 1. The inlet temperature and flow rate were measured with a sampling frequency of approximately 3Hz. These details enable a computational reconstruction of the experimental apparatus. Input error can be quantified by propagating the distribution of the input uncertainty by ASME standard methods [11].

Table 1: Conditions ranges for experimental campaign.

Flow rate (m ³ /s)	Test section T (°C)	Reservoir T (°C)	Obstruction porosity ¹
1.88x10 ⁻⁴ to 6.28 x10 ⁻⁴	250-300	200	4%-100%

¹ Several experiments include a variable-porosity obstruction to mimic the upper internal structures of an SFR, but such configuration is not discussed in this work.

In turbulent flow, model error can pose a major source of uncertainty [4]. Model error, or model inadequacy, occurs when the equations do not accurately represent the physics. For example, calculating planetary orbits using Newtonian mechanics introduces model error because the equations do not adequately account for relativity. In a similar fashion, CFD turbulence models do not fully capture all the physics of the Navier-Stokes equations, and this introduces solution error. In the sodium stratification experiment two models are present: one for turbulent momentum transfer, and one to predict turbulent heat transfer. Both could introduce errors in the final simulation results.

In a steady-state CFD simulation the averaged Navier-Stokes equations are solved to determine time-averaged velocity and pressure throughout the computational domain. A turbulence model such as the two-equation k - ϵ model is commonly applied to approximate the effect of turbulent fluctuations as an added viscosity, and this system is named Reynolds Averaged Navier Stokes (RANS). Accurately estimating this “turbulent viscosity” is the focus of two-equations RANS turbulence modelers. In a transient scenario such as the sodium stratification experiment, a time-dependent framework is required. The classic unsteady-RANS model leverages a two-equation turbulence model, with the time derivative added back to all transport equations. Time integration allows the model to resolve some large unsteady turbulent structures and predict unsteady flows like prototypical Karman vortices.

While URANS shows strong performance in many flow cases, its physical foundation is weak. The model retains the assumption, key to RANS modeling, that turbulent production and dissipation are in equilibrium. This assumption is true in steady flows, where the “turbulent cascade” follows a power law, and the large scales of turbulence are separated from the smaller scales. In regions with separation, jets, swirl, and unsteady features, this scale separation is not present, violating the assumptions in the URANS framework. In practice, URANS models often overpredicts turbulent viscosity, producing unsteady turbulent structures that are unphysically large. This can lead to erroneous predictions for local velocity, wall shear, and temperature. In the sodium stratification experiment, URANS modeling may not accurately capture inlet jet mixing or the small-scale dissipation of turbulence, both of which impact the temperature distribution.

Turbulent heat transfer also requires an engineering model. Just as turbulent velocity fluctuations transport momentum, temperature fluctuations transport heat, and their contribution must be modeled in the RANS framework. The unsteady Reynolds-averaged energy equation is given in equation 1:

$$\frac{\partial(\rho c_p T)}{\partial t} + \frac{\partial(\rho c_p T u_i)}{\partial x_i} = \frac{\partial}{\partial x_i} \left[k \frac{\partial T}{\partial x_i} - \rho c_p \overline{T' u'_i} \right], \quad (1)$$

where the term $\overline{T' u'_i}$ is the turbulent heat flux, or the time averaged product of the fluctuating velocity and fluctuating temperature. To model this term, engineers most commonly turn to the Reynolds analogy which assumes that turbulent heat flux is a diffusive process, and that the eddy diffusivity of heat is proportional to the eddy diffusivity of momentum (or the turbulent viscosity). The Reynolds analogy simplifies turbulent heat flux to equation 2,

$$\overline{T' u'_i} = - \frac{\nu_\tau}{Pr_\tau} \frac{\partial T}{\partial x_i}, \quad (2)$$

where ν_τ is the turbulent viscosity and Pr_τ is the “turbulent Prandtl number.” The Pr_τ is used to amplify or suppress turbulent heat flux until the temperature solution matches some validation criterion. In practice, most engineers use a value of 0.9, which produces adequate temperature predictions across a range of conditions [12].

However, the Reynolds analogy has clear shortcomings. For example, in a heated boundary layer of a non-unity Prandtl number fluid, the temperature and velocity gradients are not aligned, violating the assumption of proportionality between heat flux and momentum flux. Moreover, in mixed convection, mean turbulent heat flux can even flow against the mean velocity gradient, not proportional to it [13]. Consequently, model error is introduced when the Reynolds analogy is applied, and the impact of this error is not fully understood [12].

This paper demonstrates the nature of model errors in stratification simulations and motivates the development of a universal method for predicting model error in CFD heat transfer simulations.

3. METHODOLOGY

3.1 Turbulence Modeling

Due the unsteady nature of the flow in a stratification case, a transient turbulence model is required. The baseline URANS closure adopted in this study is the anisotropic k - ε model of Baglietto and Ninokata [14]. The non-linear stress strain relationship is required to capture anisotropy in the Reynolds stresses present in secondary flows, swirling, and streamline curvature. A non-constant formulation of the C_μ coefficient is used to guarantee non-negativity of the Reynolds stresses. This turbulence model has been demonstrated to accurately capture mean values and large-scale oscillations in multi-jet sodium flow [15], but its demonstration in temperature-stratified flows such is limited.

A second URANS methodology is tested and aims at addressing the limitations of URANS, including model errors associated non-equilibrium conditions. The STRUCT- ε model proposed by Xu [16] is designed to augment the URANS model with local resolution of turbulent structures and develops from the original proposal of Lenci [17]. The turbulent dissipation transport equation is given in equation 3:

$$\frac{\partial \varepsilon}{\partial t} + \bar{u}_j \frac{\partial \varepsilon}{\partial x_j} = \frac{\partial}{\partial x_j} \left[\left(\nu + \frac{\nu_\tau}{\sigma_k} \right) \frac{\partial \varepsilon}{\partial x_j} \right] + C_{\varepsilon 1} \frac{\varepsilon}{k} P_k - C_{\varepsilon 2} \frac{\varepsilon^2}{k} + \mathbf{C}_{\varepsilon 3} \mathbf{k} |\bar{\Pi}| \quad (3)$$

The last term, bolded, is the STRUCT- ε contribution to the turbulent dissipation rate. It depends on $\bar{\Pi}$, the second principal invariant of the resolved velocity gradient tensor. This term affects the viscous dissipation in areas where scale overlap is significant, suppressing turbulent viscosity in these regions. This forces the model to resolve more scales of turbulent fluctuations, rather than modeling them through the turbulent viscosity. As a result, turbulent structures approximately the size of the integral length scale are resolved. This improved resolution of the turbulence gives STRUCT- ε a significant advantage over classic URANS. In fact, STRUCT has consistently demonstrated LES-quality results with the computational cost of URANS [16].

To model heat transfer, the Reynolds analogy is applied with a constant turbulent Prandtl number of 0.9. Although there is some support for using a higher value for Pr_τ in low-Prandtl fluids, which suppresses turbulent heat flux consistent with vigorous molecular heat transfer, there is no universal guideline for the turbulent Prandtl number in mixed convection. To model buoyancy effects a temperature-dependent density relationship is applied. Sodium properties are implemented from experimental measurements [18]. All momentum and energy transport equations are integrated with a second-order nonoscillatory upwind scheme. A hybrid Gauss-least square method is used for computing reconstruction gradients, with the Venkatakrisnan's reconstruction gradient limiter; time integration is achieved with a second order accurate three time level backward Euler method.

3.2 Integral Length Scale Estimation

To estimate the integral length scale Λ in turbulent measurements along a spatial dimension r , a common approach is given by equation 4:

$$\Lambda = \int_0^{r^*} R_{ii}(r, t) dr, \quad (4)$$

where $R_{ii}(r, t)$ is the autocorrelation of the signal along r normalized by the signal variance, and r^* is the location of the first zero crossing [19]. This method is applied to estimate the length scale of temperature fluctuations along lines in the experimental and computational domain.

4. COMPUTATIONAL SETUP

4.1 Geometry and Mesh

The computational domain is reduced from the full experiment in Figure 1 to minimize computational cost. The inlets and outlets are represented as stubs in Figure 2. The experimental inlets are roughly 40 diameters downstream of a pipe bend, so they can be assumed as fully developed. In the CFD they are modeled as three fully developed pipe flow profiles, with velocity and turbulent quantities calculated from a precursor RANS simulation. The inlet temperature is interpolated directly from experimental inlet temperature measurements. The outlets are constant pressure boundaries. Conjugate heat transfer with the 5mm thick stainless steel vessel is modeled. The outer vessel surface is adiabatic, and the inner wall is a no-slip velocity condition. The upper free surface of the sodium is modeled as an adiabatic slip wall.

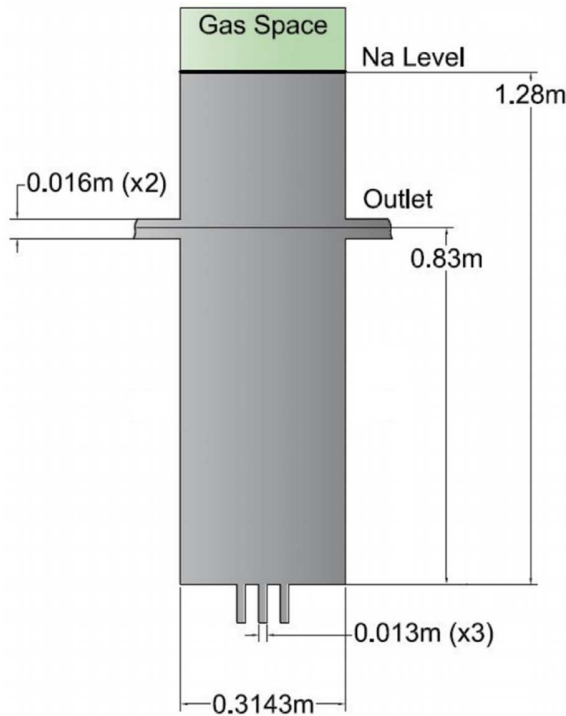


Figure 2: Test section schematic (modified from [9])

The top view in Figure 3 shows that the inlets are arranged at equal angles around the center. The odd number of jets make this flow truly 3-dimensional, with no symmetry conditions. The fiber optic temperature probes labeled in the figure extend up through the test section.

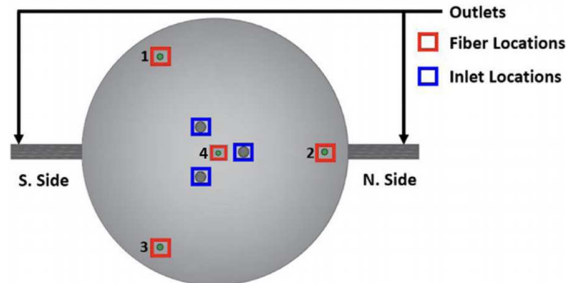


Figure 3: Top view of the test section showing the locations of inlets, outlets, and fiber optic measurement probes. The fibers are numbered consistent with the results in Figure 10

Turbulent wall effects are not expected to dominate the stratification temperature development, so wall-resolution of the turbulence equations was not implemented. Instead, a two-layer all- y^+ near wall treatment is adopted, which solves the turbulent kinetic energy up to the wall but models the near-wall turbulent dissipation with a length scale formulation. This wall treatment sacrifices some of the accuracy and flexibility of a wall-resolved approach, but the computational requirements are significantly lower.

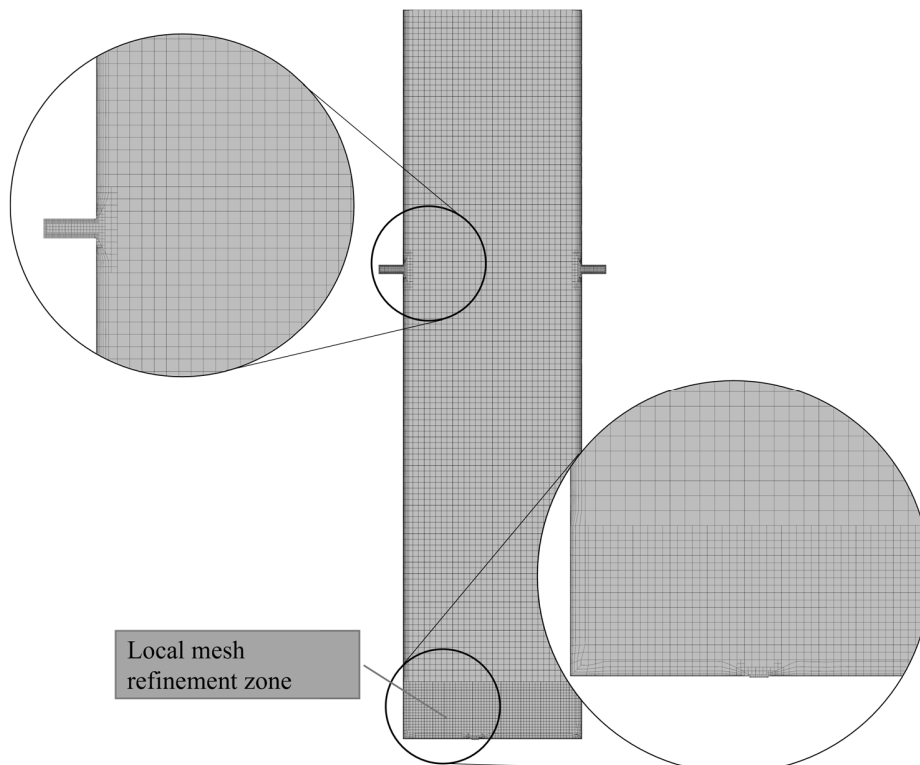


Figure 4: Computational grid with enlarged inlet and outlet details. The near-wall meshing is sized to keep the y^+ of the first cell between 1 and 20.

The computational mesh is shown in Figure 4. The model has 328,000 cells, making the full transient simulation relatively low-cost. In the lowest 0.1m of the domain a local volume refinement is applied to reduce the mesh size to 50% of the bulk size. This adds more cells in the region of highest gradients, providing a more accurate solution without dramatically increasing the cell count.

4.2 Grid Convergence

Assessing grid sensitivity and discretization error in a complex 3D unsteady simulation is challenging. A standard grid sensitivity study analyzes mean or bulk values such as pressure drop or mean velocity profile along a line. In a fully transient simulation such as the stratification experiment, no such average metric exists to measure grid sensitivity. Therefore, a simplified similar flow case is created for the grid sensitivity study.

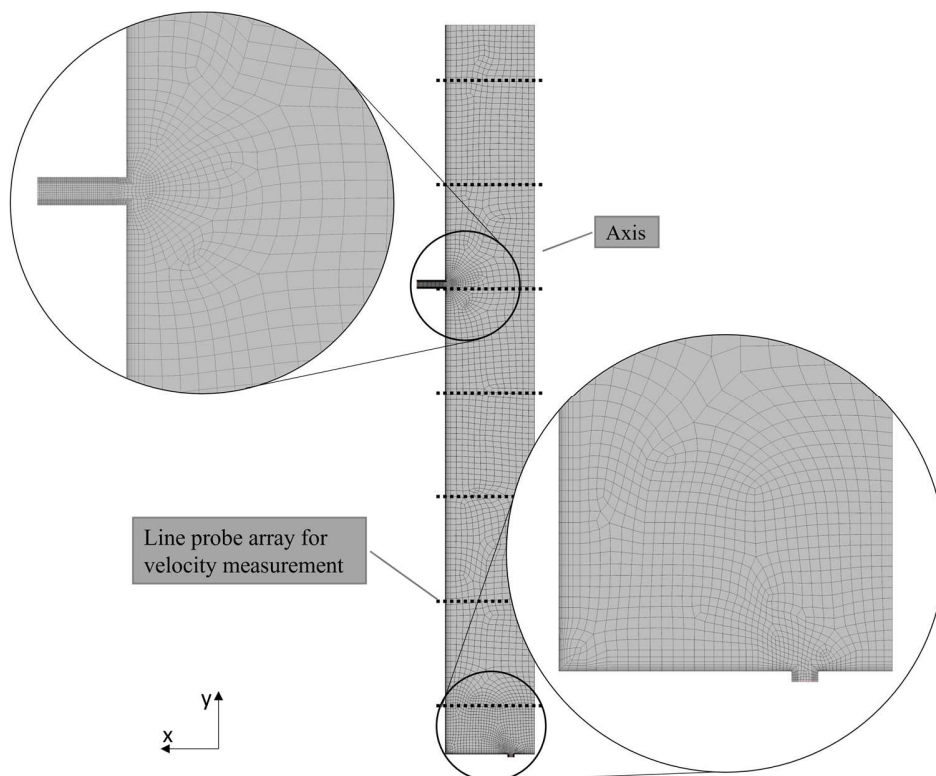


Figure 5: A view of the axisymmetric mesh for the simplified grid sensitivity simulation. The array of dashed lines indicates the position of velocity measurements in the grid sensitivity study.

The simplified case is an adiabatic, axisymmetric, steady simulation of a geometry similar to the sodium stratification experiment with the same inlet velocity. While the full 3D simulation is not steady or axisymmetric, performing grid sensitivity on the simplified case provides a credible assessment of grid effects at conditions near to the experiment, and this grid sensitivity is assumed to apply to all turbulence models studied in this work. The inlet velocity and boundary conditions are the same as the full 3D simulation, and the turbulence model is the anisotropic $k-\epsilon$ model URANS. The 2D region is computationally low-cost: grid sizes in Table 2 show the number of cells is 6,000 or less. Figure 5 shows Mesh 1. As with the full 3D mesh, a local refinement zone is included, refining the cells in the lower 0.1m to 50% of the bulk size to focus on the area with highest gradients.

Table 2: Mesh details

	Mesh base size (cm)	Number of cells
Mesh 1	1.0	6134
Mesh 2	1.25	4762
Mesh 3	1.5	3900
Mesh 4	1.75	3211
Mesh 5	2.0	3058

The metric for grid sensitivity is vertical velocity extracted at seven horizontal line probes arranged progressively up the simulation domain as noted in Figure 5. The velocity measurements plotted in Figure 6 qualitatively indicates that the area most sensitive to grid effects is the jet mixing region.

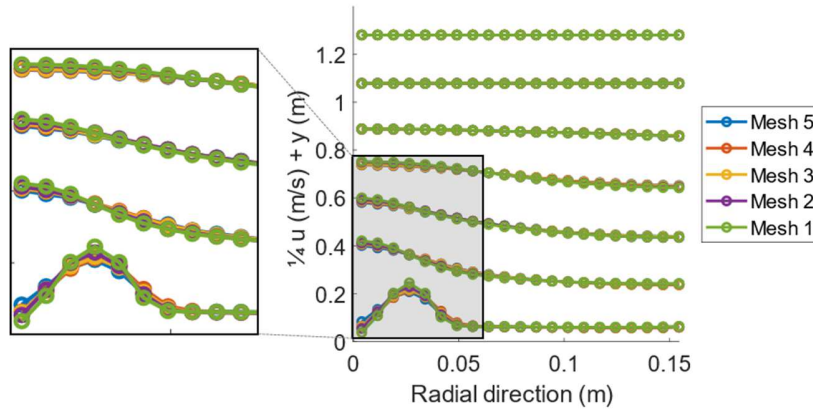


Figure 6: Vertical velocity magnitude distribution. The measurements are taken at the line probes indicated on Figure 5

Quantifying numerical error is an important step in uncertainty analysis. In this case, as with most complex mixing studies, grid convergence is oscillatory, i.e., not monotonic with grid size. To estimate the discretization error in these cases the method of Eça and Hoekstra is implemented [20]. The linear unweighted extrapolation algorithm is selected due to the relatively low standard deviation of the fit, and the discretization error estimation is presented in Figure 7 (L). As expected, the areas of higher error are near the inlets where jet mixing is sensitive to grid size. However, in most of the domain including the upper region where stratification occurs, the discretization error is low. To further quantify discretization error, Figure 7 (R) plots a cumulative error distribution. This plot demonstrates that for roughly 80% of the domain the discretization error is less than 0.05m/s. Compared to the bulk inlet velocity of approximately 1m/s, this error is small (5%), justifying the use of a mesh with a 1cm base size. The 1cm size is applied to the full 3D simulation, shown in Figure 4, with the assumption that discretization error will be similarly small.

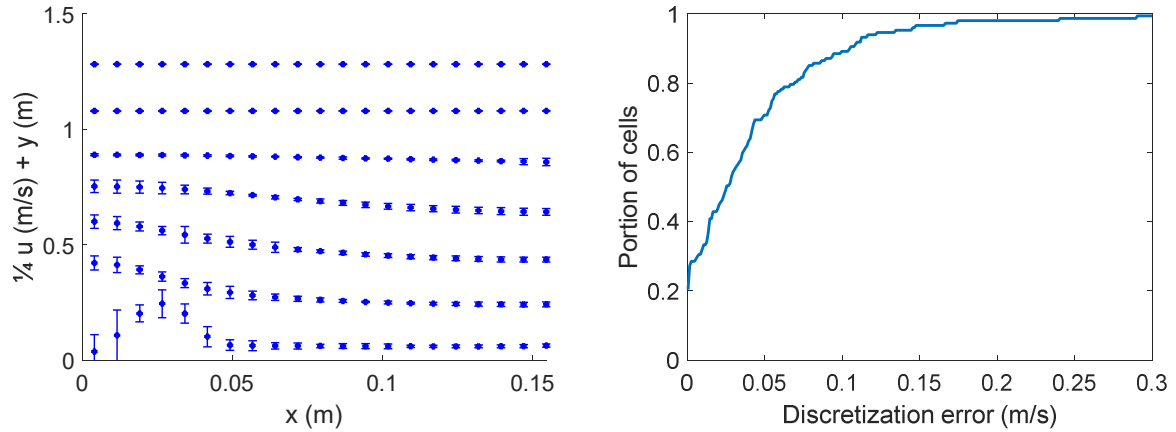


Figure 7: Left: velocity magnitude distribution from Mesh 1, with discretization error quantified as error bars. Right: cumulative error distribution confirms that the largest errors are confined to a small portion of the domain.

5. RESULTS

5.1 Qualitative Flow Descriptions

The two turbulence models, anisotropic k - ϵ URANS and STRUCT- ϵ , can be compared at any point in the transient simulation. Figure 8 is a snapshot of the turbulent structures to detail certain qualitative features of the turbulence models. URANS is expected to capture large-scale features well but STRUCT- ϵ has the advantage of resolving finer scales of turbulence in locations where unsteadiness and scale separation are dominant. This behavior is evident in the contours of the Q -criterion, or the second principal invariant of the velocity gradient. The surface of $Q=0$ is the equilibrium between vorticity and strain, which is useful for visualizing turbulent momentum structures. The results show a finer resolution of turbulence throughout the domain by the STRUCT- ϵ model.

The temperature field plotted in Figure 9 shows evidence of similar differences in scale between the URANS and the STRUCT- ϵ simulations. The temperature distribution of the URANS clearly shows the location of the cool jets, but far from the jets the temperature field is quite diffused. This is evidence of high turbulent viscosity, which boosts the modeled flux of momentum, and also the modeled turbulent heat flux due to the Reynolds analogy. The temperature distribution of the STRUCT- ϵ simulation is much more fine-scaled. In addition, the STRUCT- ϵ temperature mixing reaches higher into the stratified area above the outlets, likely due to momentum mixing by turbulent structures transported up from the jets. The lower part of the STRUCT- ϵ domain shows an additional interesting feature: fluid at higher temperature appears “trapped” in the corners of the domain. Compared with the URANS simulation, this is likely evidence of reduced modeled turbulent heat and momentum flux due to the lower turbulent viscosity.

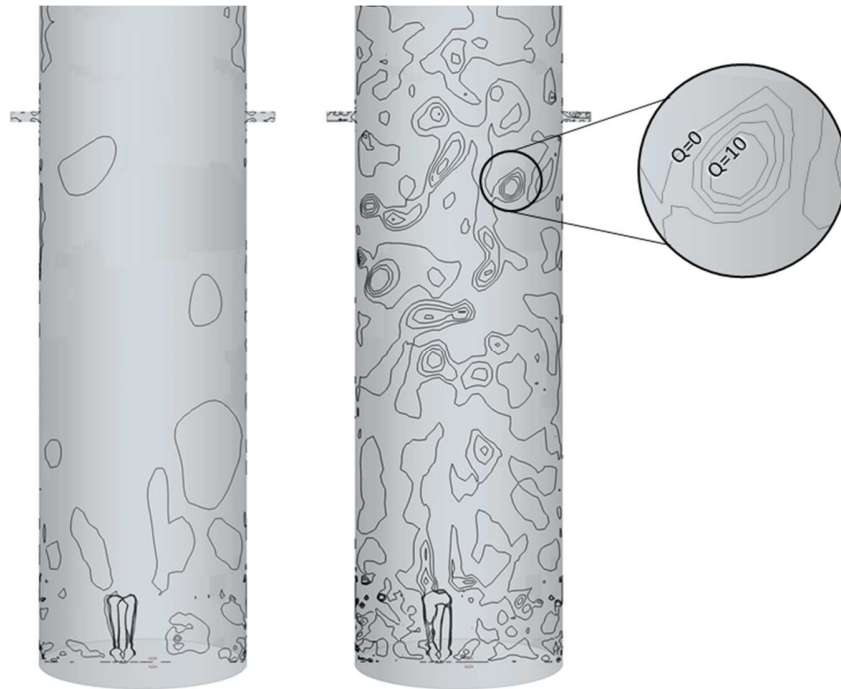


Figure 8: Contours of the Q-criterion at $t=20$ seconds on the center plane show the fine-scaled turbulent structures resolved by Struct- ϵ (R), compared to the oversized, diffused structures predicted by the URANS (L)

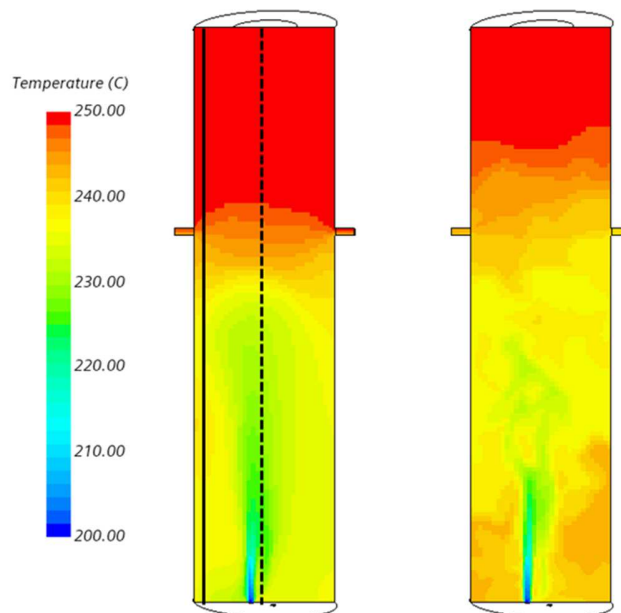


Figure 9: Temperature distribution at $t=70$ s, URANS (L) and STRUCT- ϵ (R). The upper stratified region and lower corners show significant differences. The solid line represents Fiber 2, and the dashed line represents Fiber 4.

5.2 Local Temperature Comparisons

To quantitatively compare the turbulence models with the experiment, a few metrics are presented. First, Figure 10 shows temperature plotted along the fiber optic measurement probes. As in Figure 9, the turbulence models differ in temperature magnitude near the top and bottom of the domain, and they also differ in predicting the fineness of spatial variations. This behavior is typical across the full transient. On Fibers 1-3, the STRUCT- ϵ results are closer to experiment near the bottom of the domain, avoiding the homogeneous temperature profile predicted by the URANS. This difference can be explained by the excessively diffusive URANS predicting high turbulent viscosity, which artificially amplifies shear and increases turbulent heat flux. Near the top of the domain, where the fluid stratifies, the STRUCT- ϵ model is closer to the experimental result because STRUCT- ϵ transports turbulent structures up to this location where they cause momentum mixing at the location of the stratified front.

5.2.1 Boundary condition sensitivity

The temperature predictions in the CFD simulation can be quite sensitive to certain simplifications in the boundary conditions. In Figure 10, the temperature near the outlets is particularly sensitive to the outlet geometry. To eliminate this sensitivity, the outlet stub length was increased until the temperature results stopped changing. In addition, the flow solution is quite sensitive to the smoothness of the surface mesh in the outlet stubs. The surface mesh size was decreased until the temperature solution stopped changing.

Finally, heat transfer is sensitive to the selection of boundary conditions, including conjugate heat transfer with the experiment walls. Because the test is initiated after the vessel has reached a uniform temperature at 250C, the walls will release some of the heat to the fluid as the experiment cools down. In addition, the walls conduct some heat vertically across the stratified region. This heat transfer influences the fluid temperature near the walls, and the temperature predictions are sensitive at the locations of Fibers 1-3. To achieve physically accurate temperature results, modeling the walls with conjugate heat transfer was an important part of the analysis.

5.2.2 Ensemble averaging discussion

In Figure 10, an ensemble average of the experimental temperature measurements at Fibers 1-3 is presented. Plotting the average temperature in this way is useful because it reduces the focus on random oscillations caused by turbulent structures. The experimental ensemble average and standard deviation are compared with the circumferentially-averaged CFD temperature measurements at the radial position of Fibers 1-3. As depicted in Figure 3, Fiber 2 is closer to the outlet than Fibers 1 and 3. Therefore, the ensemble average is not perfectly physical; small differences in the flow conditions are expected around the fibers near the axial position of the outlets. However, the experimental temperature standard deviation, shown in Figure 10, is not particularly large at the position of the outlet (0.83 m). This means that the ensemble average is a useful tool for comparing simulations to experiment, despite not being perfectly consistent.

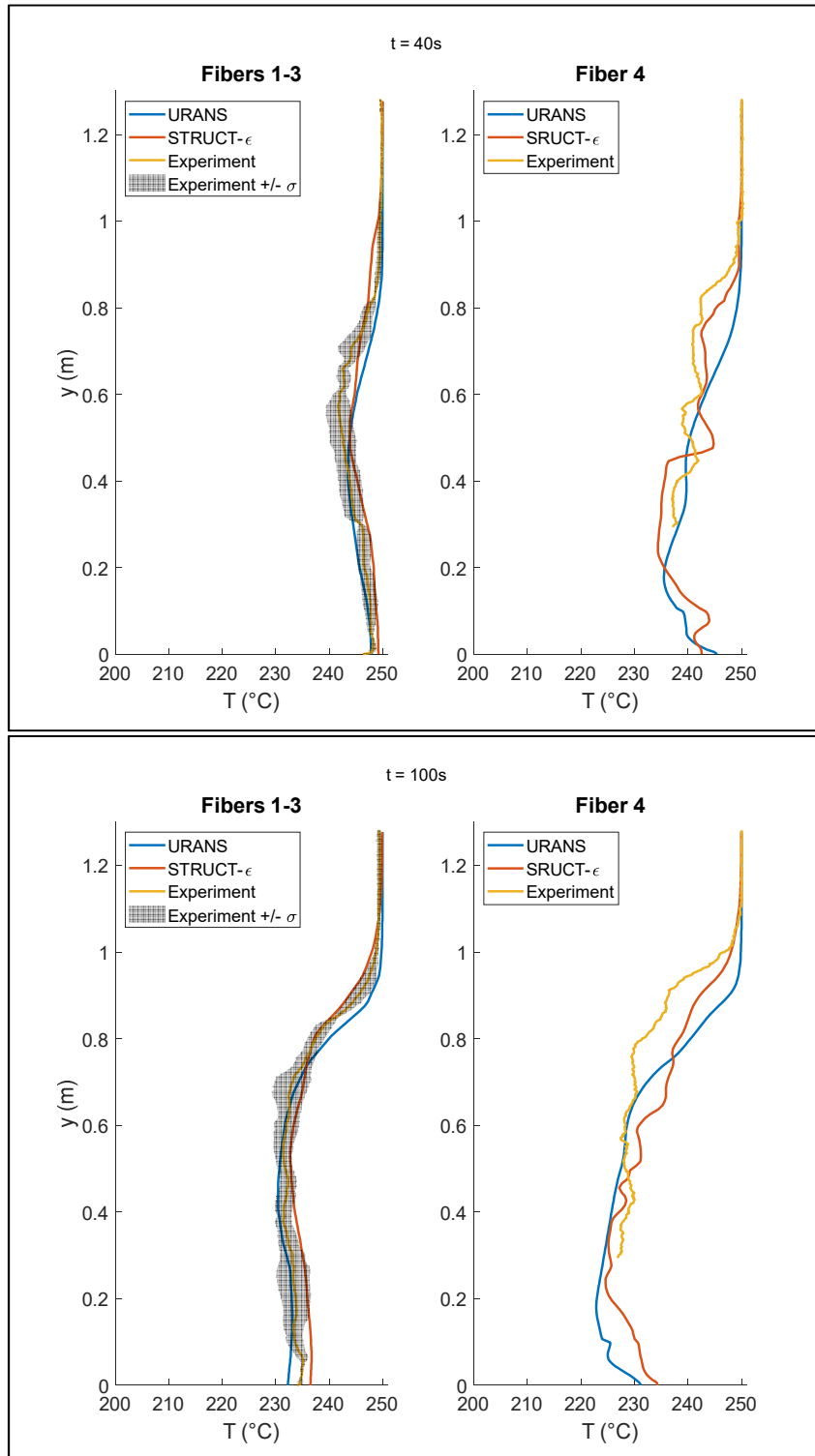


Figure 10: Temperature comparison snapshot at two times during the experiment. At left, the circumferential average temperature in the simulations is compared with the ensemble average of experiment temperature on Fibers 1-3, plus/minus the fiber temperature standard deviation. At right is the domain center comparison (Fiber 4). Fiber locations are indicated in Figure 3.

5.3 Global Error Measures

To compare the relative error across the full simulation, Figure 11 (L) plots the L_2 norm of the difference between the local temperature measurements in simulation and experiment at fibers 1-4. Early in the transient the turbulence models perform very similarly, but as low-temperature fluid reaches further into the domain the STRUCT- ϵ error is significantly lower. Natural fluctuations in temperature caused by unsteady turbulent structures cause the L_2 measure to fluctuate.

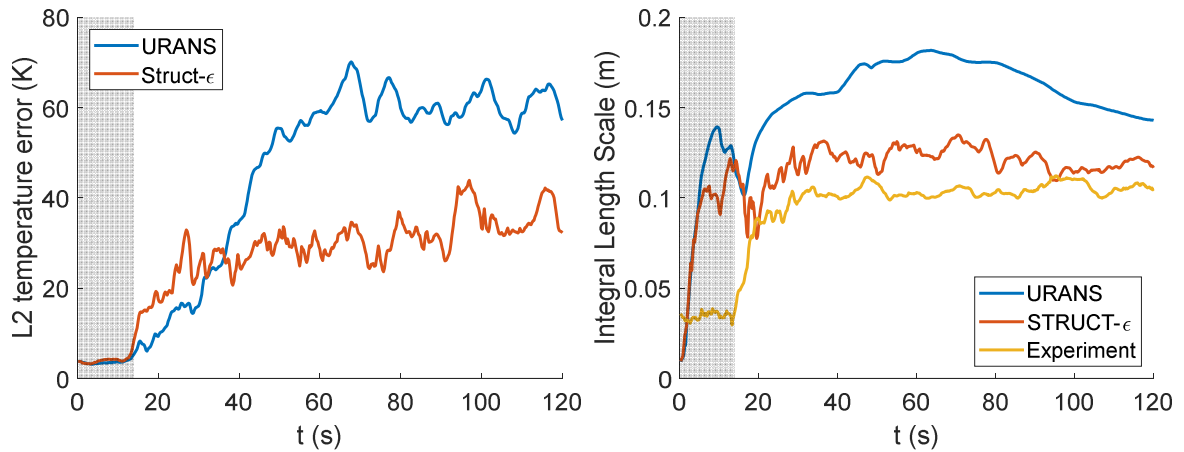


Figure 11: Left: L_2 norm of the discrepancy between simulation and experiment vs time, showing improved global performance by the STRUCT- ϵ model. Right: length scale estimation quantifies the finer scales resolved by STRUCT- ϵ . Cold sodium begins to enter the domain at the end of the grey shaded region.

Quantifying the scale of the fluctuations is another useful comparison between experiment and simulation. This length scale is directly related to the time scale of temperature oscillations, which is a key output for CFD predictions of phenomena such as thermal striping. Equation 4 is used to estimate the length scales of the temperature distribution along each fiber optic line. The mean of the length scale is plotted vs. time in Figure 11 (R). This analysis shows that the length scale predicted by STRUCT- ϵ is only 10% greater than the experiment, while the length scale of the URANS is approximately 50% larger. This finding is consistent with the expectation that URANS resolves turbulent structures that are unphysically large. Consequently, STRUCT- ϵ may perform better in thermal striping simulations where mixing length scale is related to temperature fluctuation time scales, a key component of thermal striping analysis.

6. CONCLUSIONS

Stratified sodium flow was analyzed to aid the validation of CFD methods for advanced reactor design. The sources of error in stratified flow problems are discussed: input error, numerical error, and model error. Input error is expected to be minimal given the careful geometrical recreation of experimental components and boundary conditions. Discretization error is quantified, with vertical velocity error at or below 5% of the bulk inlet velocity in 80% domain, and mostly concentrated in the lower portion of the domain below the stratification zone. Additional errors are ascribed to the engineering models of turbulent momentum and heat transfer. Future work could focus on predicting the location and magnitude of model errors.

The second-generation hybrid turbulence model STRUCT- ϵ and the cubic k- ϵ URANS are compared against experiment. STRUCT- ϵ provides significant improvement over the URANS model in terms of the absolute value of the temperature and the length scale of temperature variations. These improvements support the use of the hybrid model in liquid metal stratification simulations where accurate values of temperature and fluctuation time scales are important, such as thermal striping analysis and peak fuel temperature predictions.

ACKNOWLEDGEMENTS

This work was partially supported by the DOE Center for thermal-fluids application in nuclear energy, under agreement S001256-USDOE This material is based upon work supported by the National Science Foundation Graduate Research Fellowship under Grant No. 1745302.